

Complex Valued Sphere Decoding with Element-wise Selective Prescreening for General Two-dimensional Signal Constellations

Hwanchol Jang, Saeid Nooshabadi, *Senior Member, IEEE*, Kiseon Kim, *Senior Member, IEEE*, and
Heung-No Lee*, *Senior Member, IEEE*

Abstract—Sphere decoding (SD) is a promising detection strategy for multiple-input multiple-output (MIMO) systems because it can achieve maximum-likelihood (ML) detection performance with a reasonable complexity. The standard and most SD algorithms operate on real valued systems. These real valued SDs (RV-SDs) are known to be applicable to MIMO communication systems with only rectangular QAM signal constellations. In addition to this restriction on applicable constellations, RV-SDs are not suitable for VLSI implementations. Complex valued SD (CV-SD) is a good SD candidate for its flexibility on the choice of constellations and its efficiency in VLSI implementations. But, the low complexity CV-SD algorithm for general two dimensional (2D) constellations is not available, especially with the one that attains the ML performance. In this paper, we present a low complexity CV-SD algorithm, referred to as Circular Sphere Decoding (CSD) which is applicable to arbitrary 2D constellations. CSD provides a new constraint test. This constraint test is carefully designed so that the element-wise dependency is removed in the metric computation for the test. As a result, the constraint test becomes simple to perform without restriction on its constellation structure. By additionally employing this simple test as a prescreening test, CSD reduces the complexity of the CV-SD search. We show that the complexity reduction is significant while its ML performance is not compromised. We also provide a powerful tool to estimate the pruning capacity of any particular search tree. Using this tool, we propose the Predict-And-Change (PAC) strategy which leads to a further considerable complexity reduction in CSD.

Index Terms—multiple input multiple output (MIMO), circular sphere decoding (CSD), predict and change (PAC), sphere decoding (SD), complex valued, arbitrary constellation

I. INTRODUCTION

SPHERE decoding (SD) is a promising multiple-input multiple-output (MIMO) detection strategy because it can achieve the error rate of maximum-likelihood (ML) detector

with significantly less complexity compared to the straight-forward ML detector [1]–[4]. The standard and most SDs are real valued SDs (RV-SDs) which are only directly applicable to real valued systems. For the usages of RV-SDs, the complex valued system is decomposed into its real and imaginary parts, and it becomes a real valued equivalent system with twice the dimension of its complex valued counterpart. Here note that SD assumes each substream of data modulated independently. This independency is kept for its real valued equivalent system model when each substream is modulated by rectangular QAMs. Pham *et al.* [5] and Mozos and Garcia [6] stated that the application of RV-SD is permissible only for rectangular QAMs because otherwise invalid candidates may arise during the search; it is because the independency between the substream is broken.

It is desirable for an SD to be applicable directly on complex valued systems in the senses of *i)* its flexibility on the choice of signal constellations and *ii)* its efficiency in VLSI implementations. *i)* Complex valued SDs (CV-SDs), which are applicable directly on complex valued systems, do not require the decomposition of the systems, and the limitation of rectangular QAM can be eliminated. Each substream of data can be modulated using any two dimensional (2D) constellations. There are many constellations which are desirable to be employed in terms of many aspects of communications performance over rectangular QAMs. The benefits include the reduction in peak-to-average power ratio (PAPR) at each transmit antenna, SNR efficiency, and the increased range of choice for its data rate. To list a couple of examples, star QAM reduces the PAPR [7], and near-Gaussian constellations give the shaping gain [8], [9]; rectangular QAMs depart significantly from these constellations. *ii)* The throughput of SD VLSI implementation is inversely proportional to the product of the number of visited nodes and the time complexity for each visit of node; we assume that one node is visited for each cycle. Burg *et al.* found that the expected number of nodes visited in the SD search is nearly doubled when a complex valued system is decomposed into its equivalent real valued system [10]. For the compensation for the increase, it requires the time complexity for each visit in RV-SD to decrease to half of its CV-SD version. However, the time complexity of RV-SD is almost the same to that of CV-SD [10]. They conclude that CV-SD is appropriate for high throughput VLSI implementations [10].

This paper was presented in part at the Asilomar Conference on Signals, Systems and Computers, Pacific Grove, CA, November 2011.

Hwanchol Jang, Kiseon Kim and Heung-No Lee are with the School of Information and Communications, Gwangju Institute of Science and Technology, Gwangju, 500-712 Korea, e-mail: {hcjang, kskim, heungno}@gist.ac.kr. The asterisk * indicates the corresponding author.

Saeid Nooshabadi is with the Department of Electrical and Computer Engineering and the Department of Computer Science, the Michigan Technological University, Houghton, MI, 49931, e-mail: saeid@mtu.edu.

In CV-SDs, however, the main operation of SD, the pruning test is hard. The test relies on partial Euclidean distance (PED) computations. Here, PED computations are hard, actually the most cost expensive operations in SD, and thus, the CV-SD has high complexity. In previous CV-SDs, it is considered to restrict the applicable constellation to *i*) those whose elements are aligned in concentric rings with different radii [5], [6], [10], [11], *ii*) those whose elements are aligned with several vertical or horizontal lines [12], and *iii*) rectangular QAMs [13] for complexity reduction. Nevertheless, the general CV-SD without restriction on its constellation is still remained to be cost expensive.

It is our goal in this paper, therefore, to develop a low complexity CV-SD for general 2D constellations. We aim to do this while guaranteeing the ML performance. To this end, we take a new approach which takes advantage of a simple necessary condition, rather than an equivalent one, of the original pruning constraint, the sphere constraint (SC). We generate the necessary condition such that the metric for the constraint test becomes the magnitude of a scalar, not the Euclidean distance of a vector, thus the constraint test becomes very simple. We propose to use the necessary condition for complexity reduction in the CV-SD. The proposed constraint and the proposed CV-SD algorithm employing the constraint are referred to as the circular constraint (CC) and circular sphere decoding (CSD), respectively. CSD employs a two-step constraint test. In the prescreening step, those constellation points which are not promising are eliminated by the simple CC tests. The pruning by SC tests, in the second step, requiring expensive PED calculations is performed only for those candidates which are composed of the surviving constellation points in the CC tests. Thus, many expensive PED computations are avoided. Significant savings in the complexity of the CV-SD can be made with CSD without sacrificing the ML performance. We also propose the Predict-And-Change (PAC) strategy which further utilizes CC and reorganize the tree so that the pruning around the root is increased. This leads to a substantial complexity reduction in CSD.

The rest of this paper is organized as follows. In Section II, the system model is presented. In Section III, the underlying principle in SD, and the difference between RV-SD and CV-SD are studied. In Section IV and V, the proposed CSD algorithm and the proposed PAC strategy are developed. In Section VI, the complexity analysis for the proposed CSD is given. In Section VII, we discuss the system simulation results. Section VIII concludes the paper.

II. SYSTEM MODEL AND NOTATION

We consider a complex valued baseband MIMO channel model with m receive and n transmit antennas ($m \geq n$). Consider the system model,

$$\mathbf{r} = \mathbf{H}\bar{\mathbf{s}} + \mathbf{v}, \quad (1)$$

where $\mathbf{r} \in \mathbb{C}^m$ denotes the received signal, $\mathbf{H} \in \mathbb{C}^{m \times n}$ denotes the $m \times n$ block Rayleigh fading channel matrix whose entries

are independent and identically distributed (i.i.d.) circularly-symmetric complex Gaussian (CSCG) random variables $\mathcal{CN}(0,1)$, $\bar{\mathbf{s}} \in \mathcal{O}^n \subset \mathbb{C}^n$ is the transmitted symbol vector where $\mathcal{O} := \{o_1, o_2, \dots, o_L\}$ can be any discrete 2D constellation set with size L ; $o_i \in \mathbb{C}$ for $1 \leq i \leq L$. The components of $\bar{\mathbf{s}}$ are i.i.d. and take the values uniformly from \mathcal{O} , $\bar{s}_k \in \mathcal{O}$, and they are scaled to have $E|\bar{s}_k|^2 = 1$ for $\forall 1 \leq k \leq n$. The $m \times 1$ vector $\mathbf{v} \in \mathbb{C}^m$ is the additive noise whose entries are i.i.d. CSCG random variables $\mathcal{CN}(0, \sigma^2)$. The channel \mathbf{H} is assumed to be known at the receiver.

Variables that denote vectors and matrices are set, respectively, lowercase and uppercase boldface. $\mathbf{H}_{k,-}$ and $\mathbf{H}_{-,j}$ denotes the k^{th} row and the j^{th} column of matrix \mathbf{H} , respectively. \mathbf{H}^* and \mathbf{H}^\dagger denote the conjugate transpose and the pseudo-inverse of \mathbf{H} , respectively. Each component of a matrix or a vector is denoted by the subscript. For example, $H_{i,j}$ and s_k are the (i,j) component of \mathbf{H} and, the k^{th} component of \mathbf{s} , respectively. $\mathbf{s}_{k:n}$ is the vector taking the last $n - k + 1$ components of \mathbf{s} . $|\mathcal{O}|$ denotes the cardinality of the set \mathcal{O} . $|a|$ denotes the magnitude of $a \in \mathbb{C}$. $\|\mathbf{s}\|$ denotes the 2nd norm of vector \mathbf{s} . \mathbb{R} and \mathbb{C} denote the real and the complex domains respectively. $\Re(s_k)$ and $\Im(s_k)$ denote the real and the imaginary parts of s_k respectively. $(a)_+$ is a if $a > 0$, and 0 otherwise.

III. STUDY ON SPHERE DECODING PRINCIPLE

In this section, we describe the SD principle and the complexity problem in CV-SD.

A. SD principle

The standard procedure of SD is *i*) to identify all the candidates \mathbf{s} which satisfy the sphere constraint (SC), and *ii*) to choose the candidate with the minimum distance to the received signal \mathbf{r} as the solution. The SC is expressed by

$$\|\mathbf{r} - \mathbf{H}\mathbf{s}\|^2 \leq C, \quad (2)$$

where $\mathbf{s} \in \mathcal{O}^n$. But, this is not efficient for implementation. For a better implementation, the SC can be expressed as

$$\begin{aligned} d_k(\mathbf{s}_{k:n}) &:= \sum_{i=k}^n |y_i - \mathbf{R}_{i,i:n} \mathbf{s}_{i:n}|^2 \\ &= d_{k+1}(\mathbf{s}_{k+1:n}) + |b_{k+1}(\mathbf{s}_{k+1:n}) - R_{k,k} s_k|^2 \leq C, \end{aligned} \quad (3)$$

for $1 \leq k \leq n$ where \mathbf{R} is the upper triangular matrix from the QR decomposition of \mathbf{H} , $\mathbf{H} = \mathbf{Q}\mathbf{R}$, $\mathbf{y} := \mathbf{Q}^* \mathbf{r}$, $d_{n+1} = 0$, and $b_{k+1}(\mathbf{s}_{k+1:n}) := y_k - \mathbf{R}_{k,k+1:n} \mathbf{s}_{k+1:n}$. Here, $d_k(\mathbf{s}_{k:n})$ is referred to as partial Euclidean distance (PED) and it depends on the partial vector $\mathbf{s}_{k:n}$, the last $n - k + 1$ components of \mathbf{s} , which is associated with the nodes at the k^{th} level of the tree. As PED is

monotonically increasing as k decreases, PEDs for the remaining levels of k do not need to be computed once PED of a level is found to violate the SC in (3). This gives computational savings to SD. As a result, SDs provide complexity reductions for ML solution search.

Definition 1: (element-wise independent metric) We call a metric is *element-wise independent* if the metric at a level of tree, say the k^{th} level, depends only on the value of the corresponding element s_k in \mathbf{s} but not on that of any s_i where $i \in \{1, 2, \dots, n\}$ and $i \neq k$. Note that this element-wise independence is different from the statistical independence between two random variables.

Here, we should note that the SC tests in (3) are still hard as the PEDs are element-wise dependent. Assume that the value of s_i for any $1 \leq i \leq n$ changes, the PED of the k^{th} level of the tree for level $k \leq i$ need to be calculated again. This increase the required number of PED computations and the cost for each PED computation exponentially as k decreases. In the past, a simplified SC where explicit PED computations are not required, rather than the SC in (3), was employed for a lower complexity algorithm. Further simplification on SC was obtained, as noted in the introduction, by employing rectangular QAMs and exploiting the characteristics that exists in the constellations, e. g., the independence between the real and the imaginary components.

B. The difference between RV-SD and CV-SD

In real valued systems where the components of \mathbf{r} , \mathbf{H} , $\bar{\mathbf{s}}$, \mathbf{s} , and \mathbf{v} are real valued, the SC of (3) can be simplified by the so called admissible interval (AI) which is expressed by the lower limit s_k^l and the upper limit s_k^u as follows

$$s_k \in [s_k^l, s_k^u], \quad (4)$$

where $s_k^l = \frac{b_{k+1}(\mathbf{s}_{k+1:n})}{R_{k,k}} - \frac{\sqrt{C-d_{k+1}(\mathbf{s}_{k+1:n})}}{R_{k,k}}$ and $s_k^u = \frac{b_{k+1}(\mathbf{s}_{k+1:n})}{R_{k,k}} + \frac{\sqrt{C-d_{k+1}(\mathbf{s}_{k+1:n})}}{R_{k,k}}$.

The AI is still element-wise dependent since $b_{k+1}(\mathbf{s}_{k+1:n})$ and $d_{k+1}(\mathbf{s}_{k+1:n})$, for the AI at the k^{th} level of the tree, are functions of $\mathbf{s}_{k+1:n}$, other than s_k . But it can be identified by calculating only the two values, s_k^l and s_k^u . The SC of (4) is used in RV-SD instead of the SC of (3) for it is simpler. The constellation points s_k which satisfy the SC can now be identified without explicit PED computations $d_k(\mathbf{s}_{k:n})$ of candidates $\mathbf{s}_{k:n}$ for the current level k of the tree. PED computations are needed only for the nodes in the AI in RV-SD. They are not for pruning itself but for setting the AI, s_{k-1}^l and s_{k-1}^u , for the next level of the tree. However, please note that, the AI simplification of the SC applies only to rectangular QAMs. Refer to [2]-[4] for more conceptual description of RV-SD.

In this work, the aim is for a CV-SD for general 2D constellations. This makes it difficult to replace the expensive operations for the SC in (4) with cheaper operations. Hence, every single pruning in the CV-SD is done by the explicit

expensive PED computations for the SC test (3) [10]. This results in high complexity in the CV-SD. Let us see the difference on the number of PED computations of the CV-SD and the RV-SD, and the numbers of the floating point operations (FLOPs) of them. Consider a tree which is used for the SD search. The tree expands with the factor L as the level of the tree, k , goes down, starting from $k = n$ to $k = 1$. The number of nodes at the k^{th} level of the tree is L^{n-k+1} and each node represents a candidate for the partial vector $\mathbf{s}_{k:n}$. Assume that there are N_{k+1}^{sc} nodes which satisfy the SC at $(k+1)^{\text{th}}$ level of the tree. In the CV-SD, all the children nodes of the surviving nodes are calculated for their PEDs. That is $L \cdot N_{k+1}^{\text{sc}}$ PED computations for the k^{th} level of the tree. We name this *L-expansion property* of the CV-SD. This property is trivial but it will be easier for us to recall this property later on. In the RV-SD, only the N_k^{sc} nodes which are inside the AI are required for PED computations at the k^{th} level of the tree no matter how large N_{k+1}^{sc} is. Surely, $L \cdot N_{k+1}^{\text{sc}} \geq N_k^{\text{sc}}$. The respective FLOPs of the PED computations for CV-SD and for RV-SD are $(6(n-k)+8L)N_{k+1}^{\text{sc}}$ and $(2(n-k)+4)N_k^{\text{sc}}$.¹ Actually, the direct comparisons of the numbers of the PED computations and those of the FLOPs are not fair for the system models for RV-SD and for CV-SD are different. But, at least, we can see the inefficiency of the CV-SD for it includes $L \cdot N_{k+1}^{\text{sc}}$ factor rather than N_k^{sc} .

For low complexity CV-SDs, Hochwald and Brink [11], Burg *et al.* [10], Pham *et al.* [5], and Mozos and Garcia [6] consider restricting the applicable signal constellations only to those whose elements are aligned in several concentric rings with different sizes, rather than general 2D constellations, so that they can exploit the constellation structure. An AI is obtained for these complex valued constellations. There, the interval is not for the value of s_k itself but for its phase $\angle s_k$. Obviously the applicability of the method is limited to only those constellations with the specific shape. In addition, it requires costly trigonometric function and other computations. In this paper, we do not consider this approach. Note also that the one in [14] considers a fixed complexity realization of CV-SD. It reduces the complexity for general CV-SD. But we also do not consider this in this paper since it sacrifices the ML performance for its complexity.

C. Schnorr-Euchner enumeration

In Schnorr-Euchner (SE) enumeration, the children nodes of

¹ Computation of $b_{k+1}(\mathbf{s}_{k+1:n})$ requires $(n-k)$ complex multiplications and $(n-k)$ complex additions, totaling $6(n-k)$ FLOPs (one complex multiplication and one complex addition are equivalent to four FLOPs and two FLOPs, respectively). The remaining computation for the PED computation in (3) requires 8 FLOPs. The computation of $b_{k+1}(\mathbf{s}_{k+1:n})$ is required only once for it is common for the candidates as it does not depends on s_k . For RV-SD, computation of $b_{k+1}(\mathbf{s}_{k+1:n})$ requires $2(n-k)$ FLOPs and the remaining computation requires 4 FLOPs. Note that one more FLOP is required in case of a SC test for a comparison with C ; consider this in Sec. IV-A.

a parent node are visited in the ascending order of their PEDs during the search. Once a preceded child node is found to violate the SC, it is definite that the remaining siblings also violate the SC and they do not need to be searched. This provides a considerable complexity reduction to SD.

In RV-SD, the sorting can be made without explicit PED computations of the siblings. The first sibling s_k is determined by slicing $\frac{b_{k+1}(\mathbf{s}_{k+1:n})}{R_{k,k}}$ to the closest constellation point. The sequence of the remaining siblings is then determined by the zigzag ordering of the neighboring constellation points of the first sibling [2]. Thus, the SE enumeration in RV-SD can be done very efficiently.

With the best knowledge of the authors, there is no efficient SE enumeration scheme for the CV-SD which is applicable to arbitrary 2D constellations and achieves the exact ML performance; we consider this in this paper. Thus, the SE enumeration for the CV-SDs requires explicit PED computations for all the siblings. Note that there are several efficient SE or SE-like enumeration schemes [5], [6], [10], [12], [13], [15]. But, they are for the CV-SDs which *i*) limit their constellations to certain kinds and exploit the special structures of them, and/or *ii*) compromise the exact ML performance. *i*): Pham *et al.* [5], Mozos and Garcia [6], and Burg *et al.* [10] apply SE enumerations on the constellations whose elements are aligned in several concentric rings with different sizes. The SE enumeration by Hess *et al.* [12] partitions the constellation into subsets consisting of rows or columns and reduces the enumeration overhead. But, this is efficient only for the constellations most of whose elements are aligned with several vertical or horizontal lines. Mennenga and Fettweis [13] aim to exploit the symmetry of rectangular QAM constellations for efficient SE enumeration. *ii*): The SE-like method by Wenk *et al.* [15] uses approximations, such as the l -1 norm or the so called l -infinity norm, of the PED for efficient enumeration. In this method, the remaining siblings are pruned once a preceded sibling node is found to violate the SC as they are in other SE enumerations. This may prune the node from which the ML solution originated; they use an approximation, not the PED itself.

IV. PROPOSED CIRCULAR SPHERE DECODING

The applicability to general 2D constellations is an important benefit of the general CV-SDs. But, this generality gives an inherent problem in the CV-SD. No structure of a specific constellation can be exploited for a simplification of the SC in (3). This makes it difficult to have a simpler but equivalent constraint to the SC.

In this section, we simplify the SC of (3) by resorting to one of its necessary conditions, rather than to any specific structure in constellations. We refer to the necessary condition as the circular constraint (CC). Since the CC is a necessary condition, it may not prune as tightly as the SC may. Not to lose any pruning efficiency in the CV-SD, SC tests are executed for those nodes which are not eliminated by the preceded CC tests. We call this CV-SD employing CC tests circular sphere decoding

(CSD). CSD prunes the nodes the same amount as the baseline CV-SD does but with a smaller number of SC tests. Here, CSD is efficient since the cost for CC tests is small. It is because CC is derived so that the element-wise dependency inside the norm calculation in (3) is removed.

A. Circular constraint (CC)

SC tests in (3) is hard due to the element-wise dependence of the PEDs. Now, we aim to find a new constraint where the element-wise dependence of the metric is removed. We start from the SC in (3). The element-wise dependency is removed by eliminating the matrix \mathbf{R} inside the norm operator. The derivation is given by

$$\begin{aligned} C &\geq d_k(\mathbf{s}_{k:n}) \\ &= \|\mathbf{R}_{k:n,k:n}(\mathbf{x}_{k:n} - \mathbf{s}_{k:n})\|^2 \\ &= \frac{\|\mathbf{H}_{k,-}^\dagger\|^2}{\|\mathbf{H}_{k,-}^\dagger\|^2} \|\mathbf{R}_{k:n,k:n}(\mathbf{x}_{k:n} - \mathbf{s}_{k:n})\|^2 \\ &\stackrel{(a)}{\geq} \frac{|\mathbf{R}_{k,k:n}^\dagger \mathbf{R}_{k:n,k:n}(\mathbf{x}_{k:n} - \mathbf{s}_{k:n})|^2}{\|\mathbf{H}_{k,-}^\dagger\|^2} \\ &\stackrel{(b)}{=} \frac{|x_k - s_k|^2}{\|\mathbf{H}_{k,-}^\dagger\|^2}, \end{aligned} \quad (5)$$

where $\mathbf{x} := \mathbf{H}^\dagger \mathbf{r}$ with $\mathbf{H}^\dagger := (\mathbf{H}^* \mathbf{H})^{-1} \mathbf{H}^*$, (a) is from $\|\mathbf{H}_{k,-}^\dagger\| = \|\mathbf{R}_{k,k:n}^\dagger\|$ and the Cauchy-Schwarz inequality, and (b) is from the fact that $\mathbf{R}^\dagger \mathbf{R}(\mathbf{x} - \mathbf{s}) = \mathbf{x} - \mathbf{s}$ with the assumption that $\mathbf{H} \in \mathbb{C}^{m \times n}$ has the full rank with $m \geq n$. For a \mathbf{H} with rank deficiency, there are contributions in the metric derived in (5) from the elements of $\mathbf{x} - \mathbf{s}$ other than the k^{th} element of it. But, they are insignificant unless \mathbf{H} has serious rank deficiency.

Now, we have a new constraint, CC,

$$\Delta_k(s_k) \leq C \cdot \delta_k^2, \quad k = 1, 2, \dots, n, \quad (6)$$

where $\Delta_k(s_k) := |x_k - s_k|^2$ and $\delta_k^2 := \|\mathbf{H}_{k,-}^\dagger\|^2$. We name the metric $\Delta_k(s_k)$ as circular metric (C-metric). Here, δ_k^2 can be computed before the SD search begins and the value of δ_k^2 does not change until \mathbf{H} changes, thus it can be used while \mathbf{H} stays the same. Please note that CC is a necessary condition for a candidate \mathbf{s} to satisfy the SC. It is because the metric derived in (5) is smaller than or equal to the PED for SC in (3).

The C-metric $\Delta_k(s_k)$ is element-wise independent since it depends only on s_k (Def. 1). This element-wise independence gives CC two beneficial features in terms of complexity. First, the required number of CC tests is fixed only to L for each level of the tree. It is because the C-metric does not depend on the elements of the parent node, and hence the C-metrics for the children nodes originated from one parent node are the same with those from any other parent nodes. Note that the number of required SC tests at the k^{th} level of the tree is $L \cdot N_{k+1}^{\text{sc}}$ (Sec. III-B); this ranges from L to L^{n-k+1} . Second, each CC test is

simple. A CC test requires only six FLOPs while a SC test requires $6(n-k)+9$ FLOPs for the first sibling at the k^{th} level of the tree and 9 FLOPs for the remaining siblings.¹ Thanks to these two features, the CC tests at the k^{th} level of the tree require only $6L$ FLOPs while the SC tests require $(6(n-k)+9L)N_{k+1}^{\text{sc}}$ FLOPs.

Note that there are some lower bounds used in other SDs [16], [17]. Stojnic *et al.* provide several lower bounds on the remaining path metric using ideas from H^∞ estimation theory and some of its special cases [16]. Barik and Vikalo obtain a lower bound on the metric by relaxing the metric minimization problem [17]. But, it is difficult to utilize them for prescreening on the SC tests because *i)* they are not lower bounds on the current PED but on the remaining path metric and *ii)* they are computationally expensive due to their element-wise dependency; they require $b_{k+1}(\mathbf{s}_{k+1:n})$ in the metric computations.

B. Circular sphere decoding

In CSD, we utilize the simple CC for prescreening on the SC tests, thus reduce the computational complexity of the search. The strategy in CSD is *i)* to eliminate nodes as many as possible for a given level of the tree using the CC, and then *ii)* to perform SC tests only for the surviving nodes.

Consider Fig. 1 where we specify the CSD operations by providing the geometry of the CC and the SC. The CC is represented in the \mathbf{s} space by n separate circles, one for each element of \mathbf{s} . The SC is represented by the sphere in the $\mathbf{H}\mathbf{s}$ space. In the prescreening step of CSD, the constellation points which are not inside each separate circle are excluded in the search. In the pruning step, the process of identifying vector points which are inside the sphere is performed. This process requires SC tests. But, these SC tests are performed only for the prescreened candidates. In CSD, many not promising candidates are eliminated in the prescreening test even before

their SC tests are performed. As it is shown in Fig. 1, only a portion of the points are pruned by the SC tests in CSD (Fig. 1 (b)), while whole pruning operations in the CV-SD are solely through the SC tests. Thus, the employment of the CC test in CSD reduces the complexity of the CV-SD. As a result, CSD outperforms the CV-SD in terms of complexity (Section VII). Note that the ML performance in CSD is not compromised since the CC test does not eliminate the ML solution; the CC is necessary for a candidate for the satisfaction of the SC.

Note that the proposed CSD can employ statistical pruning techniques such as those in [18]-[20] for additional complexity reduction. This can be done just by replacing the C by one of those proposed in [18]-[20].

The entire algorithm of the proposed CSD is given in Table I.

C. Circular enumeration

SE enumeration has a distinct benefit in reducing the complexity of the search. But, the SE enumeration for general CV-SDs is not suitable for CSD for its heavy overhead. Fortunately, there are C-metrics available in CSD. C-metric of a node is a kind of a lower bound on the PED of the node (Eq. (5)). Thus, it can be used as a surrogate PED for the purpose of efficient enumeration.

We sort the constellation points in non-decreasing order with respect to their C-metrics as follows,

$$s_k^1, s_k^2, \dots, s_k^L \text{ s. t. } \Delta_k(s_k^1) \leq \Delta_k(s_k^2) \leq \dots \leq \Delta_k(s_k^L). \quad (7)$$

This provides a benefit of making more nodes be pruned by efficient CC tests. The CC becomes stricter whenever the search proceeds and reaches toward a leaf in the tree; the radius is reduced to the metric of the leaf. Now that the siblings are sorted by the C-metric, stricter CC tests are performed for those siblings which have higher chances of getting pruned by the CC, with larger C-metrics. This makes more candidates eliminated before the SC tests. It is shown in Sec. VII that the CSD with the circular enumeration (C-CSD) provides considerable

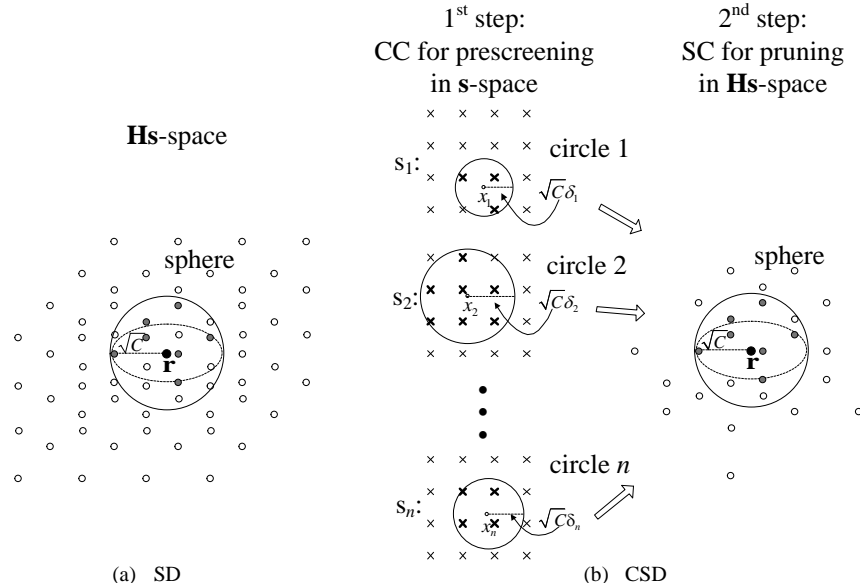


Fig. 1. Geometry of SD and the proposed CSD with 16 QAM constellation (gray-colored points represent those points which are inside the sphere). (a) SD. (b) CSD.

complexity reduction to CSD; it also outperforms the SE-SD.

TABLE I

The CSD Algorithm	
Definitions:	$\mathcal{O} = \{o_1, o_2, \dots, o_L\}$ (the constellation set), $\delta^2 = [\delta_1^2, \delta_2^2, \dots, \delta_n^2]^T$, k (the current level), C (squared radius), $\mathbf{s} = [s_1, s_2, \dots, s_n]^T$ (the currently visited node), d_k (the PED for the current level), $\hat{\mathbf{s}}$ (ML solution). Inputs: \mathcal{O} , δ^2 , C_0 , \mathbf{r} , \mathbf{x} , and \mathbf{R} . Outputs: $\hat{\mathbf{s}}$. Step 0: (C-metric) Compute C-metrics $\Delta_k(s_k)$ for $\forall s_k \in \mathcal{O}$ and $\forall k$. Step 1: (Initialization) set $C \leftarrow C_0$, $k \leftarrow n$, $found \leftarrow 0$. Step 2: (Initialization of the node for a visit) for $k = 1 : n$ set $I_k = 1$ and $s_k = o_1$. end Go to step 4 Step 3: (Next node) if $I_k \neq L$, set $I_k = I_k + 1$ and $s_k = o_{I_k}$, and go to step 4 else go to step 8 Step 4: (CC test *) if $\Delta_k(s_k) \leq C \cdot \delta_k^2$, go to step 5 else go to step 3 Step 5: (PED) Compute PED $d_k(s_{kn})$. Step 6: (SC test) if $d_k(s_{kn}) < C$ go to step 7 else go to step 3 Step 7: (Forward) if $k = 1$, $C \leftarrow d_k$ (radius updates), $\hat{\mathbf{s}} \leftarrow \mathbf{s}$, $found \leftarrow 1$, go to step 3. else $k \leftarrow k - 1$, go to step 4 Step 8: (Backward) if $k = n$ (root node) if $found = 0$, $C_0 \leftarrow C_0 + \Delta C_0$ (radius increase), go to step 2 else exit else for $k' = 1 : k$ set $I_{k'} = 1$ and $s_{k'} = o_1$. end $k \leftarrow k + 1$, go to step 3

* $C \cdot \delta_k^2$ is not computed for every CC test. It is computed only when the radius C is updated in Step 7.

V. PROPOSED PREDICT-AND-CHANGE STRATEGY

Pruning of a single node at a level of a tree amounts to pruning of the whole sub-tree underneath it whose size in the number of nodes is exponential to the number of levels left to go. It is thus efficient in CSD, and in other SDs, to prune nodes at higher levels of the tree. Aiming to increase pruning at higher levels of the tree, we take the approach which *i*) predicts the pruning potential of each symbol s_i of \mathbf{s} for $1 \leq i \leq n$, and *ii*) reorganizes the tree so that the symbols with larger pruning potentials to be placed at higher levels of the tree; the CSD

search is performed on this tree. In the following subsection, we develop the idea of pruning potential for each symbol and provide a method to calculate it.

A. Symbol pruning potential

The pruning potential we propose to use here is an upper bound on the number of constellation points that can be pruned by the CC test. The largest number of constellation points that can be pruned by the CC test is calculated by using the strictest CC test which prunes as many constellation points as possible but without pruning the ML solution. Of course, this requires the identification of the ML solution or the distance between the ML solution and the received signal \mathbf{r} , which are not available until the CSD search is completed. We instead obtain an upper bound on the largest number of constellation points. This can be calculated by using the concept of the minimum circles. Note that there is no computationally feasible way to predict a non-trivial upper bound on the number of nodes that can be pruned by the SC test prior to a SD search.

Definition 2: (the minimum circles) The minimum circles (MCs) are the n smallest circles *i*) which are centered at x_1, x_2, \dots, x_n , respectively, *ii*) the proportion of whose radii is $\delta_1 : \delta_2 : \dots : \delta_n$, and *iii*) each of which contains at least a single constellation point inside it; the ML solution is not always included in the vector points \mathbf{s} which are constituted by the constellation points inside the circles.

Let us denote the set of constellation points inside the i^{th} circle of the MCs by $\mathcal{O}_i^{\text{MC}}$. $\mathcal{O}_i^{\text{MC}}$ can be identified by using the following proposition.

Proposition 3: A constellation point $s_i \in \mathcal{O}$ belongs to $\mathcal{O}_i^{\text{MC}}$ if and only if

$$\Delta_i(s_i) \leq C_{\min} \cdot \delta_i^2, \quad (8)$$

where $C_{\min} := \max_i \left\{ \delta_i^{-2} \min_{s_i \in \mathcal{O}} \Delta_i(s_i) \right\}$.

Proof: The minimum radius for each circle of the MCs is $\delta_i^{-2} \min_{s_i \in \mathcal{O}} \Delta_i(s_i)$ for $1 \leq i \leq n$. The maximum radius is selected to guarantee that all the circles in MCs contain at least a constellation point inside. \square

The MCs are the geometric view of the strictest CC test which is satisfied by at least one of $\mathbf{s} \in \mathcal{O}^n$. The CC test corresponding to the MCs is stricter than or equal to the strictest CC test which the ML solution satisfies. Thus, we can obtain the pruning potential, an upper bound on the number of constellation points that can be pruned by the CC test, for each symbol as follows

$$P_i := L - \left| \mathcal{O}_i^{\text{MC}} \right| = \left| \left\{ s_i \mid \Delta_i(s_i) > C_{\min} \delta_i^2, s_i \in \mathcal{O} \right\} \right|, \quad (9)$$

for $1 \leq i \leq n$.

B. Predict-And-Change (PAC) strategy

The pruning potential P_i for each symbol s_i for $i = 1, 2, \dots, n$ in \mathbf{s} can be obtained using (9) once the C-metrics are computed

for a received signal \mathbf{r} . Using the pruning potentials, the symbols of \mathbf{s} and the columns of \mathbf{H} are reordered. We propose that the n symbols in \mathbf{s} are placed from the root ($k = n$) to the leaf ($k = 1$) of the tree in non-increasing order with respect to their pruning potentials. The n columns in \mathbf{H} are also reordered correspondingly. The reordered \mathbf{s}' and \mathbf{H}' are constituted as follows,

$$\begin{aligned} \mathbf{s}' &= [s_{i_1}, s_{i_2}, \dots, s_{i_n}]^T \\ \text{and } \mathbf{H}' &= [\mathbf{H}_{\cdot i_1}, \mathbf{H}_{\cdot i_2}, \dots, \mathbf{H}_{\cdot i_n}] \\ \text{s. t. } P_{i_1} &\leq P_{i_2} \leq \dots \leq P_{i_n}. \end{aligned} \quad (10)$$

Then, the reorganized search tree is created by doing the QR decomposition on \mathbf{H}' . The CSD search is performed on the reorganized tree; the reorganization is done right before Step 1 in TABLE I.

Different from the SD ordering schemes which consider only \mathbf{H} [2], [4], PAC exploits the information of the received signal \mathbf{r} . Remember that this becomes possible in PAC because it is based on the pruning potentials which are available prior to the formation of a tree. It is shown in Fig. 2 that the complexity reduction in CSD which employs the PAC strategy (PAC-CCSD) is substantial compared to that with the conventional ordering (PINV-CCSD); this conventional ordering places symbol with a smaller inverse channel norm $\|\mathbf{H}_{\cdot i_n}^\dagger\|^2$ at a higher level of the tree.

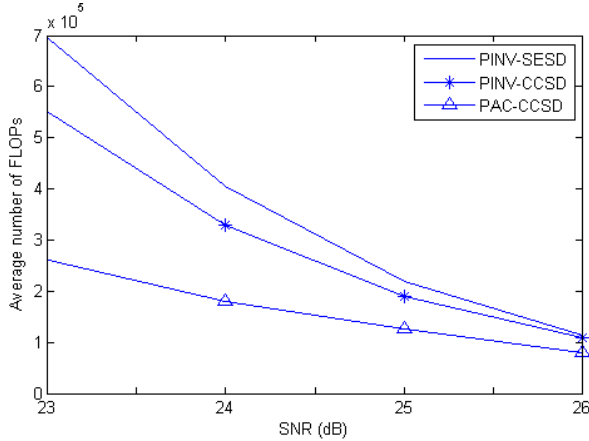


Fig. 2. Complexity of PAC-CCSD, PINV-CCSD, and PINV-SESD for 10×10 MIMO systems with 64 QAM.

C. A modified PAC

QR decompositions in SDs need to be performed whenever the channel \mathbf{H} changes. For PAC strategy, it requires n factorial QR decompositions per channel change since there exist n factorial different reordered channel matrices \mathbf{H}' . This may not be any problem in terms of computational overhead when the channel changes slowly (quasi-static channel), but otherwise, it may become problematic.

We here provide a variation of PAC and reduce the computational overhead of QR decompositions. This reduces the overhead per channel change significantly while the benefit of PAC per channel use is still kept large. For the variation, we consider a subset of \mathbf{H}' , only n different reordered channel

matrices \mathbf{H}' out of the total n factorial of them. The reorganization is modified as follows,

$$\mathbf{s}' = [s_{i_1}, s_{i_2}, \dots, s_{i_n}]^T$$

$$\text{and } \mathbf{H}' = [\mathbf{H}_{\cdot i_1}, \mathbf{H}_{\cdot i_2}, \dots, \mathbf{H}_{\cdot i_n}] \quad (11)$$

$$\text{s. t. } i_n = \arg \max_{i_k} \{P_{i_k}\} \text{ and } \delta_{i_1}^2 \geq \delta_{i_2}^2 \geq \dots \geq \delta_{i_{n-1}}^2.$$

The root of the tree, $k = n$, is placed by the symbol with the largest pruning potential. The other levels of the tree from $k = n-1$ to $k = 1$ are placed by the remaining symbols in non-decreasing order with respect to their δ_i^2 .

Although the pruning potentials are utilized only for the symbol to be placed at the root and δ_i^2 is utilized instead for the other levels of the tree, the benefit of PAC is reduced only slightly (Sec. VII). The intuition for this is that *i*) we use the pruning potential at the level with the best pruning efficiency and *ii*) for other levels, we still consider pruning potentials but in the average sense since a smaller δ_i^2 indicates a larger P_i in the case where the information of $\Delta_i(s_i)$ and C_{\min} is not available (refer to (9)).

It is now possible with these n QR decompositions to give a comparable complexity reduction to that of the n factorial QR decompositions. In addition, we provide in the following subsection an efficient way of performing the n QR decompositions and the computational overhead is reduced to be less than that of two QR decompositions. With the modification and the efficient QR decompositions, we can say that the problem of PAC with the computational overhead is resolved.

D. Computational overhead for the modified PAC

We assume that Givens rotation, a well-known unitary transform based method, is used for QR decompositions. We do not consider the Gram Schmidt method here for it requires costly operations, square root operations and divisions, and it is not numerically stable; see [21] and references therein.

There are mainly two kinds of operations in Givens rotation, rotation and cancellation. Rotation makes a complex valued element turned into a real valued one. Cancellation makes a real valued element annihilated. For each columns of \mathbf{H}' , rotations and cancellations are performed. For the k^{th} column, $\mathbf{H}'_{\cdot k}$, the elements $H'_{i,k}$ for $k \leq i \leq n$ are rotated and become real valued. Here, the complexity for rotations for the column is $(n-k+1) \cdot C_{\text{rot}}(n-k+1)$ where $C_{\text{rot}}(n-k+1)$ is the computational complexity for a rotation for the k^{th} column. Note that the single rotation for $H'_{i,k}$ amounts to the rotations for the $n-k+1$ elements, $H'_{i,j}$ for $k \leq j \leq n$, since the operations corresponding to the rotation for $H'_{i,k}$ are performed to those elements $H'_{i,j}$ where $k+1 \leq j \leq n$.

Once the rotations are done, the elements $H'_{i,k}$ for $k+1 \leq i \leq n$ which now have turned into real valued ones are annihilated and zero valued. Here, the complexity for

cancellations for the column is $(n-k) \cdot C_{\text{can}}(n-k+1)$ where $C_{\text{can}}(n-k+1)$ is the computational complexity for a cancellation for the k^{th} column. Note also that the single cancellation for $H'_{i,k}$ amounts to the cancellation for the $n-k+1$ elements for the same reason with the rotations. Now, the diagonal element $H'_{k,k}$ becomes real valued and the lower diagonal elements becomes zero. By performing the rotations and the cancellations from the 1st column to the n^{th} column of \mathbf{H}' , a QR decomposition is done. The cost of this operation is $C_{\text{QR}} = \sum_{k=1}^n (n-k+1) \cdot C_{\text{rot}}(n-k+1) + (n-k) \cdot C_{\text{can}}(n-k+1)$.

There are n QR decompositions required for the proposed variation of PAC. This may be done by performing n separate QR decompositions; this costs nC_{QR} . Fortunately, this can be done very efficiently (with less than $2C_{\text{QR}}$) by *i*) performing a QR decomposition on \mathbf{H}' whose columns are ordered by δ_i^2 and *ii*) deriving remaining $n-1$ QR decompositions from the one in '*i*'. For the explanation of the method, let us assume that $\delta_1^2 \geq \delta_2^2 \geq \dots \geq \delta_n^2$. We use \mathbf{H}'_{i_n} for the denotation of the reorganized \mathbf{H} by (11). For '*i*', in this case, $i_n = n$, a separate QR decomposition is performed. And for the remaining QR decompositions, the upper triangular matrix \mathbf{R}'_n obtained in '*i*' is used instead of \mathbf{H}' . For the case of $i_n = i$, the i^{th} column of \mathbf{R}'_n is placed at the most right position, and the columns from the $i+1^{\text{th}}$ to the n^{th} positions are shifted to the left by one. Then, the QR decomposition for $i_n = i$ can be made with only $C_i = \sum_{k=i}^n C_{\text{rot}}(n-k+1) + \sum_{k=i}^{n-1} C_{\text{can}}(n-k+1)$. This is done for $i_n = 1, 2, \dots, n-1$. Then, the net computational overhead for the n QR decompositions becomes $C_{\text{net}} = C_{\text{QR}} + \sum_{k=1}^n k \cdot C_{\text{rot}}(n-k+1) + (k-1) \cdot C_{\text{can}}(n-k+2) < 2C_{\text{QR}}$.² An example for the QR decompositions is given in Fig. 3.

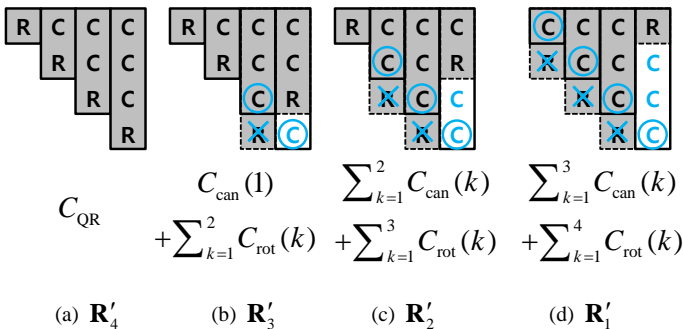


Fig. 3. Efficient QR decompositions for $n=4$. The capital letters R and C in the matrix are meant to imply that the element in the pertinent position is either real or complex valued respectively. The circles and crosses are to represent the rotations and the cancellations, respectively. Gray colored rectangles are the columns taken from the upper triangular matrix in (a).

² The computation overhead for \mathbf{Q} matrix generation is not discussed here. However, it is still $C_{\text{net}} < 2C_{\text{QR}}$ for the computational overhead for \mathbf{Q} matrix generation is proportional to the number of rotations and cancellations.

VI. COMPLEXITY ANALYSIS

In this section, we aim to analyze the complexity of the proposed CSD in Sec. IV-B. We use FLOPs as a measure of complexity. A lower bound on the expected FLOPs as function of n and SNR is analyzed. On the one hand, a lower bound analysis could be undesirable if the bound is not tight. But, on the other hand, the final expression of the lower bound could be simple enough to give a clear insight. To rip the benefit of the latter, we take the lower bound approach in this paper. We found that the lower bound can still give useful information on the additional complexity reduction behavior of CSD to that of the CV-SD. There are other lower bound analyses in the literature, those by Jaldén and Ottersten [22] and Shim and Kang [19]. Vikalo and Hassibi provide the exact expected complexity [23], [24], and Gowaikar and Hassibi provide an upper bound [18]. But, their final results are not easy to interpret for their complex expressions as they include integrations.

A. Overview on the complexity of CSD

Let the number of nodes which satisfy the SC at the k^{th} level of the tree be called N_k^{sc} , i.e.,

$$N_k^{\text{sc}} := \left| \left\{ \mathbf{s}_{k:n} \in \mathcal{O}^{n-k+1} \mid d_k(\mathbf{s}_{k:n}) \leq C \right\} \right|, \quad (12)$$

where $d_k(\mathbf{s}_{k:n}) = \sum_{i=k}^n \left| \mathbf{R}_{i,i:n}(\bar{\mathbf{s}}_{i:n} - \mathbf{s}_{i:n}) + \tilde{\mathbf{v}}_i \right|^2$ denotes the PED of $\mathbf{s}_{k:n}$ and $\tilde{\mathbf{v}} := \mathbf{Q}^* \mathbf{v}$ is a random vector whose entries are i.i.d. CSCG random variables, and the number of nodes which satisfy the CC at the k^{th} level of the tree be called N_k^{cc} ,

$$N_k^{\text{cc}} := \left| \left\{ s_k \in \mathcal{O} \mid \tilde{\Delta}_k(s_k) \leq C \right\} \right|, \quad (13)$$

where $\tilde{\Delta}_k(s_k) := \delta_k^{-2} |x_k - s_k|^2 = \delta_k^{-2} |\bar{s}_k - s_k + \mathbf{R}_{k,-}^* \tilde{\mathbf{v}}|^2$ denotes the C-metric of s_k divided by δ_k^2 .

In CV-SD, the complexity is given by

$$C_{\text{SD-C}} = \sum_{k=1}^n (6(n-k) + 9L) N_{k+1}^{\text{sc}}, \quad (14)$$

where $N_{n+1}^{\text{sc}} = 1$. Recall the L -expansion property (Sec. III-B). That is, for the identification of N_k^{sc} nodes at the k^{th} level of the tree, $L \cdot N_{k+1}^{\text{sc}}$ PED computations are required; this results in high complexity in the CV-SD; note the L in $9L$.

In the case of CSD, the high complexity problem of the CV-SD is alleviated. Among all the possible children nodes of each surviving node at the previous level, $k+1$, note that there are L children nodes, only those children nodes, $N_k^{\text{cc}} \leq L$ of them, which satisfy the CC are passed for PED computations. The complexity for CSD is given by

$$C_{\text{CSD-C}} = \sum_{k=1}^n 6L + (6(n-k) + 9N_k^{\text{cc}}) N_{k+1}^{\text{sc}}. \quad (15)$$

Here, $6L$ is the FLOPs for the CC tests at each level.

We analyze the complexity of CSD in the following

subsection.

B. CSD complexity

The expected complexity of CSD over \mathbf{H} , $\bar{\mathbf{s}}$, and \mathbf{v} is

$$\mathbb{E}[C_{\text{CSD-C}}] = \sum_{k=1}^n 6L + 6(n-k) \cdot \mathbb{E}[N_{k+1}^{sc}] + 9 \cdot \mathbb{E}[N_k^{cc} N_{k+1}^{sc}]. \quad (16)$$

For simplicity of the derivation, we assume $m=n$ in the sequel. But, it can be easily seen that the result for the general case $m>n$ remains the same. We also use the SNR $\rho = \frac{m}{\sigma^2}$ and the radius $C = \alpha n \sigma^2$ where α is determined so that a solution is found with a high probability, $1 - \varepsilon = 0.99$, in the sphere [24]. Since the complexity is averaged over $\bar{\mathbf{s}}$, we consider $\tilde{\Delta}_k$ and d_k as functions of not only \mathbf{s} but also $\bar{\mathbf{s}}$.

Lemma 4: $\mathbb{E}[N_k^{cc} N_{k+1}^{sc}]$ is lower bounded by

$$\mathbb{E}[N_k^{cc} N_{k+1}^{sc}] \geq \frac{1}{L^{n-k+1}} \sum_{\mathbf{s}_{k:n}} \sum_{\bar{\mathbf{s}}_{k:n}} \Pr(\tilde{\Delta}_k(\mathbf{s}_k, \bar{\mathbf{s}}_k) \leq C) \Pr(d_{k+1}(\mathbf{s}_{k+1:n}, \bar{\mathbf{s}}_{k+1:n}) \leq C). \quad (17)$$

Proof: See Appendix A. \square

We compute $\Pr(\tilde{\Delta}_k(\mathbf{s}_k, \bar{\mathbf{s}}_k) \leq C)$ first, and then $\Pr(d_{k+1}(\mathbf{s}_{k+1:n}, \bar{\mathbf{s}}_{k+1:n}) \leq C)$.

Lemma 5: The probability $\Pr(\tilde{\Delta}_k(\mathbf{s}_k, \bar{\mathbf{s}}_k) \leq C)$ is lower bounded by

$$\Pr(\tilde{\Delta}_k(\mathbf{s}_k, \bar{\mathbf{s}}_k) \leq C) \geq \left(1 - \frac{1}{\alpha n} \left(\|\bar{\mathbf{s}}_k - \mathbf{s}_k\|^2 \rho + 1 \right)\right)_+. \quad (18)$$

Proof: See Appendix B. \square

Now, we compute a lower bound on $\Pr(d_{k+1}(\mathbf{s}_{k+1:n}, \bar{\mathbf{s}}_{k+1:n}) \leq C)$.

Lemma 6: The probability $\Pr(d_{k+1}(\mathbf{s}_{k+1:n}, \bar{\mathbf{s}}_{k+1:n}) \leq C)$ is lower bounded by

$$\Pr(d_{k+1}(\mathbf{s}_{k+1:n}, \bar{\mathbf{s}}_{k+1:n}) \leq C) \geq \left(1 - \frac{n-k}{\alpha n} \left(\|\bar{\mathbf{s}}_{k+1:n} - \mathbf{s}_{k+1:n}\|^2 \frac{\rho}{n} + 1 \right)\right)_+. \quad (19)$$

Proof: See Appendix C. \square

Finally, we obtain a lower bound on the expected complexity of CSD.

Theorem 7: The expected complexity $\mathbb{E}[C_{\text{CSD-C}}]$ is lower bounded by

$$\mathbb{E}[C_{\text{CSD-C}}] \geq \sum_{k=1}^n 6L + 6(n-k)(1 - \beta_s)_+ + 9L^{n-k+1}(1 - \beta_s)_+(1 - \beta_c)_+, \quad (20)$$

where

$$\beta_c := \frac{1}{\alpha n} \left(\mathbb{E}[\|\bar{\mathbf{s}}_k - \mathbf{s}_k\|^2] \rho + 1 \right) \quad (21)$$

and $\beta_s := \frac{n-k}{\alpha n} \left(\mathbb{E}[\|\bar{\mathbf{s}}_k - \mathbf{s}_k\|^2] \frac{\rho}{n} + 1 \right)$ are the complexity

reduction factors which are determined by the system parameters. Here, $\mathbb{E}[\|\bar{\mathbf{s}}_i - \mathbf{s}_i\|^2]$, the average intra-constellation squared distance, is determined when the constellation is decided; for example, it is 2 for QAMs and PSKs, and 1.8163 for (8,24,32) 64 star QAM.

Proof: See Appendix D. \square

A lower bound on the expected complexity of the CV-SD can be easily obtained by using a similar procedure, but with (14) and Lemma 6.

Theorem 8: The expected complexity $\mathbb{E}[C_{\text{SD-C}}]$ is lower bounded by

$$\mathbb{E}[C_{\text{SD-C}}] \geq \sum_{k=1}^n 6(n-k)(1 - \beta_s)_+ + 9L^{n-k+1}(1 - \beta_s)_+. \quad (22)$$

C. Special complexity reduction behavior in CSD

The objective of the analysis is to have a clear insight on the complexity reduction of CSD to that of CV-SD. To this end, we provide a lower bound on the CSD complexity in (20). A special complexity reduction behavior of CSD is estimated. Even though a lower bound is used for the evaluation, the complexity reduction behavior in simulations agrees to the analyzed one.

CSD utilizes an additional constraint, CC, in addition to SC. This results in an additional multiplicative factor in (20), $(1 - \beta_c)_+$, at the last term of the CSD complexity compared to the CV-SD complexity in (22). Among the last term in (22), β_c portion of them are excluded in (20); $()_+$ and $6L$ here are ignored for easy evaluation. We expect that this gives CSD a complexity reduction relative to the CV-SD.

We note in (21) that the additional complexity reduction factor β_c increases as *i*) SNR increases and/or *ii*) n decreases. That is, it is expected that the additional complexity reduction in CSD to the CV-SD become more as SNR increases and/or n decreases. This finding exactly matches to the complexity reduction behavior of CSD which is observed in the simulations (Fig. 4). Here, the complexity reduction behavior on n may not be attractive. But, this problem disappears when PAC is utilized; it performs better as n increases (Sec. VII).

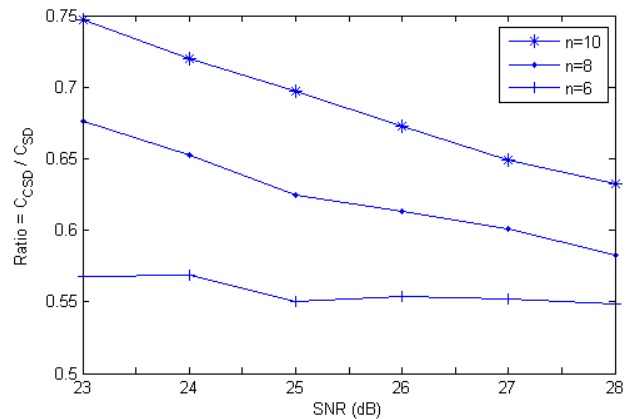


Fig. 4. Ratio of CSD complexity and CV-SD complexity for 10×10, 8×8, and 6×6 MIMO systems with 64 QAM.

Here, please note a special complexity reduction behavior of CSD that it increases as SNR increases, rather than becoming smaller. It is a unique complexity reduction behavior of CSD which has an additional constraint. For most of other low complexity SDs which are based on a (stricter) single constraint, the additional complexity reductions to the reference SDs tend to decrease as SNR increases [10], [19], [25]. At very high SNRs, the constraint tests of the both the low complexity SD and the reference SD become strict enough. And, the average complexities of them become almost the same as only one node per level survives from the constraint tests with high probability; thereby only one PED computation is required for a level of the tree for both SDs.

In CSD, CC tests reduce the complexity of the search additionally. The improved efficiency of the CC in high SNR directly applies to the additional complexity reduction capability of CSD to the CV-SD. That is why additional complexity reduction in CSD to the CV-SD becomes more as SNR increases. It is also true even at an extremely high SNR. At a glance, it seems that the complexities of the two algorithms become almost the same in the region as both the constraint tests become strict, thereby only one node per level survives in the constraint tests. But, it is not true. Even if only one node per level survives in SC tests, $N_k^{sc} = 1$, L PED computations need to be done for each level of the tree in the CV-SD because of the L -expansion property; refer to (14). Therefore, it still needs more than one PED computations per level in the CV-SD. However, even though CSD is a CV-SD, it is still possible to achieve one PED computation per level. It is because the CC tests become so strict in extremely high SNR region that only one constellation point for each element of the vector \mathbf{s} passes the test with high probability; this can be seen in (15) by letting $N_k^{cc} = 1$ and $N_k^{sc} = 1$. This makes it possible to have a larger additional complexity reduction in higher SNR regions; until the complexities of CSD and SD become so small that the term $6L$ becomes significant in (20).

VII. SIMULATION RESULTS

A. Setup

In this section, we show the complexity reduction capability of the proposed CSDs using system simulations. We compare the proposed CSDs (CSD in Sec. IV-B, C-CSD in Sec. IV-C, and PAC-CCSD in Sec. V) with the conventional CV-SDs (SD, SE-SD, and PINV-SESD) which are also directly applicable to general complex valued constellations. To show the effectiveness of the proposed CSDs in general 2D constellations, we consider star QAM, rectangular QAM, and PSK in simulations. Here, note that the usage of CSD is not limited to these three constellations; it is applicable to arbitrary complex valued constellations. We use 8×8 and 10×10 MIMO systems with (4, 24, 32) star 64 QAM for the ring ratios of (2, 3) [7],³

³ The ring ratios indicates the ratios of the minimum ring amplitude to the other ring amplitude.

rectangular 64 QAM, and 32 PSK. The initial radius is set to $C_0 = \alpha n \sigma^2$. If no solution found, the radius is increased until a solution is found [24]. During the tree search, the radius is updated whenever a candidate is found to be in the sphere radius. We employ the average FLOPs as a metric for complexity; they are averaged over 10^4 runs of channels in each SNR value. The range of SNR is determined so that the symbol error rate (SER) of order of 10^{-1} , 10^{-2} , and between them are obtained.

B. Results

We first consider star QAM. The usage of star QAM is desirable in the applications which require low PAPR, compared to rectangular QAM [7]. Fig. 5 plots the average numbers of FLOPs for the CV-SDs and the proposed CSDs in MIMO systems with (8,24,32) star 64 QAM. The proposed CSDs reduce the complexities of the CV-SDs considerably. We observe that CSD, C-CSD, and PAC-CCSD outperform SD, SE-SD, and PINV-SESD by 35%, 38%, 40%, 41%, by 32%, 31%, 26%, 17%, and by 43%, 28%, 11%, -18%, respectively, at SNR (dB) of 24, 25, 26, 27 in 8×8 MIMO systems. For 10×10 MIMO systems, CSD, C-CSD, and PAC-CCSD reduce the complexities of SD, SE-SD, and PINV-SESD by 28%, 31%, 33%, 37%, by 28%, 31%, 29%, 28%, and by 51%, 38%, 31%, 15%, respectively.

As discussed in Section VI-C, the complexity reduction factor of CSD increases as SNR increases and/or n decreases.

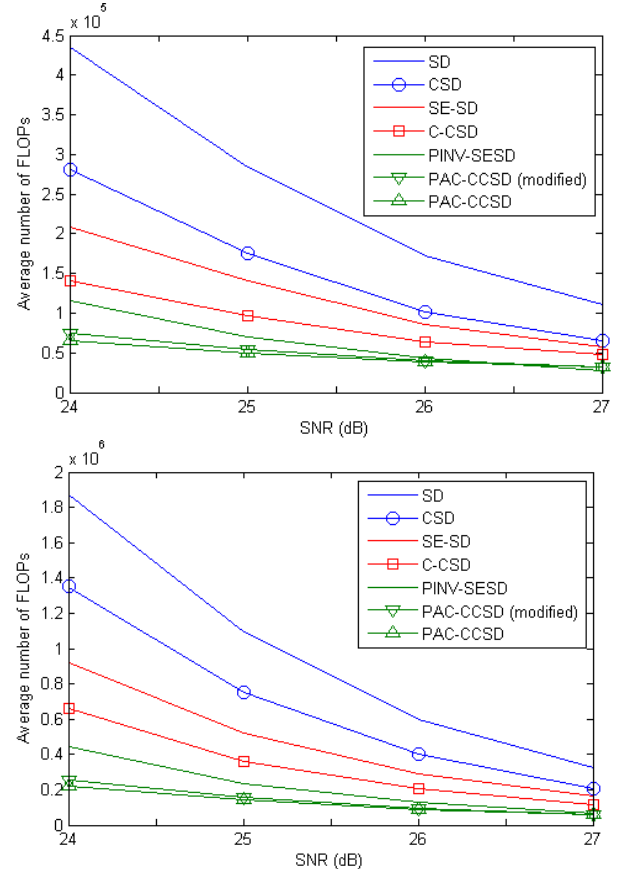


Fig. 5. Complexities of CV-SDs and the proposed CSDs for 8×8 and 10×10 MIMO systems with (8,24,32) star 64 QAM.

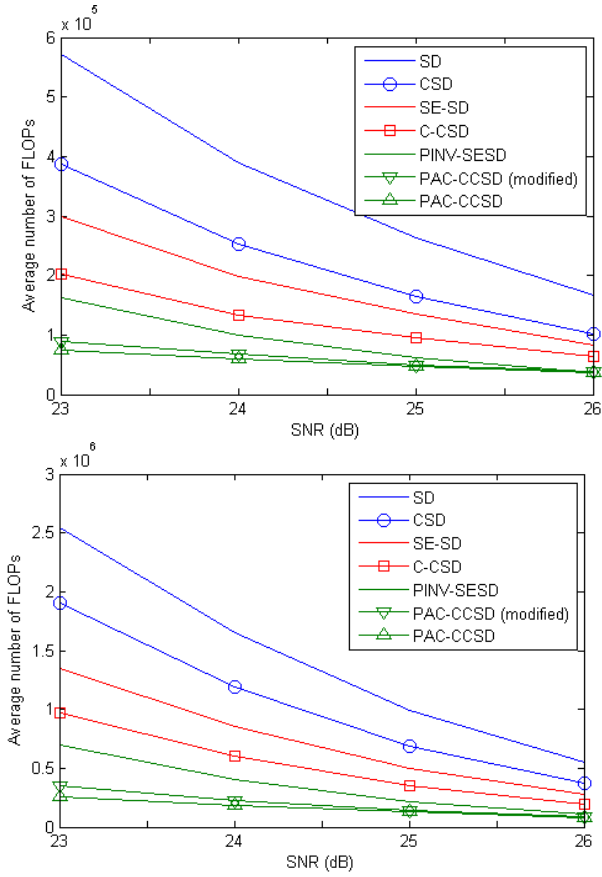


Fig. 6. Complexities of CV-SDs and the proposed CSDs for 8×8 and 10×10 MIMO systems with 64 QAM.

Interestingly, the complexity reduction factor of PAC-CCSD behaves in the opposite way to that of the CSD; it increases as SNR decreases and n increases. There are significant complexity reductions in the proposed CSDs in almost all the SNR regions (up to 41% by CSD at 27 dB and up to 43% by PAC-CCSD at 24dB in 8×8 MIMO systems and up to 37% by CSD at 27 dB and up to 51% by PAC-CCSD at 24dB in 10×10 MIMO systems). Note that these complexity reductions in CSDs are obtained without compromising its ML performance; of course, they all achieved the ML performance in simulations. It was found that PAC-CCSD has a higher complexity than PINV-SESD does at SNR of 27 dB in 8×8 MIMO system. Still, it is not a big issue since both of them have low complexities in the region.

We also consider rectangular QAM and PSK. The patterns of the complexity reduction of the proposed CSDs in rectangular QAM and PSK are similar to those in star QAM. It is observed that the proposed CSDs perform better than CV-SDs by large margins in these constellations. For 64 QAM, CSD, C-CSD, and PAC-CCSD outperform SD, SE-SD, and PINV-SESD by 32%, 35%, 38%, 39%, by 32%, 32%, 30%, 23%, and by 55%, 41%, 26%, 2%, respectively, in 8×8 system, by 25%, 28%, 30%, 33%, by 28%, 30%, 30%, 29%, and by 62%, 55%, 43%, 31%, respectively, in 10×10 system at SNR (dB) of 23, 24, 25, 26

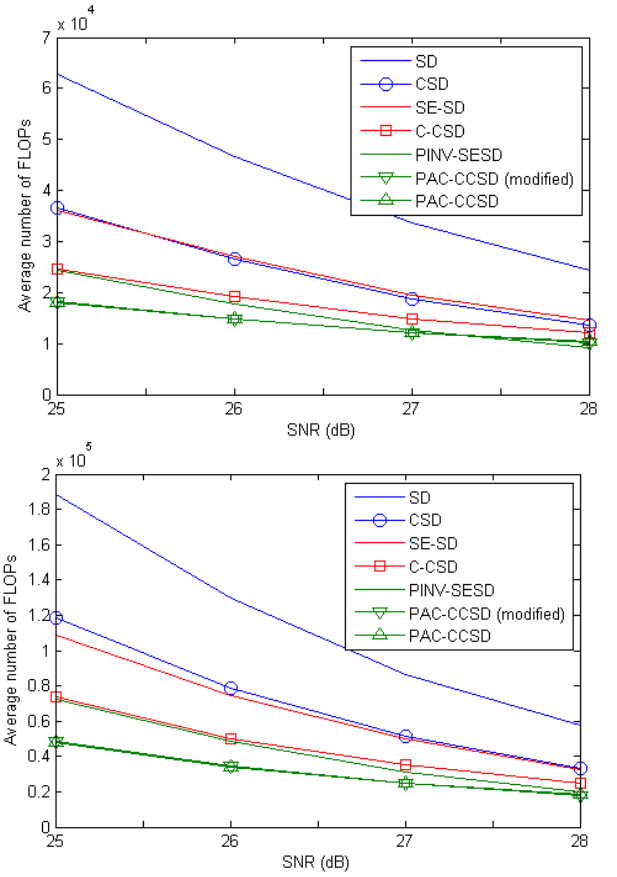


Fig. 7. Complexities of CV-SDs and the proposed CSDs for 8×8 and 10×10 MIMO systems with 32 PSK.

(Fig. 6).

For 32 PSK, the respective complexity reduction ratings of CSD, C-CSD, and PAC-CCSD from SD, SE-SD, and PINV-SESD are (42%, 43%, 44%, 45%), (32%, 29%, 24%, 17%), and (26%, 16%, 4%, -13%) in 8×8 system, (37%, 39%, 40%, 42%), (32%, 32%, 30%, 25%), and (33%, 30%, 20%, 6%) in 10×10 system at SNR (dB) of 25, 26, 27, 28 (Fig. 7).

VIII. CONCLUSION

In this paper, we have proposed CSD, a low complexity CV-SD, for general 2D constellations. CSD aims at reducing the cost of SC tests, the most computationally expensive operations in SD. It uses the simple circular constraint (CC) for prescreening candidates and pruning some of them even before executing the SC tests. In simulation, it is shown to give a large reduction in the number of FLOPs. We also propose a further complexity reduction strategy, the Predict-And-Change (PAC). PAC also provides a further considerable complexity reduction. Thanks to the proposed methods, the CSD becomes surely a good candidate for a general 2D constellation low complexity MIMO detector. Now with the proposed CSD, it becomes possible to decode signals with integer data rate (not only for $L = 2^i$, $i = 1, 2, \dots$) and arbitrary shape of 2D constellations which may be optimal for target applications with low complexity while achieving the ML performance as CSD is

compatible to general 2D constellation. Many 2D constellations can be handled in this single CSD algorithm without any additional constellation-dependent functionality.

APPENDIX

A. Proof of Lemma 4

$$\begin{aligned}
& \mathbb{E}[N_k^{cc} N_{k+1}^{sc}] \\
&= \mathbb{E} \left[\sum_{s_k} I\{\tilde{\Delta}_k(s_k, \bar{s}_k) \leq C\} \sum_{s_{k+1:n}} I\{d_{k+1}(s_{k+1:n}, \bar{s}_{k+1:n}) \leq C\} \right] \\
&= \sum_{s_{k:n}} \Pr(\tilde{\Delta}_k(s_k, \bar{s}_k) \leq C, d_{k+1}(s_{k+1:n}, \bar{s}_{k+1:n}) \leq C) \\
&\stackrel{(a)}{=} \frac{1}{L^{n-k+1}} \sum_{s_{k:n}} \sum_{\bar{s}_{k:n}} \Pr(\tilde{\Delta}_k(s_k, \bar{s}_k) \leq C, d_{k+1}(s_{k+1:n}, \bar{s}_{k+1:n}) \leq C),
\end{aligned} \tag{23}$$

where $I\{\cdot\}$ is the indicator function which is 1 for the condition inside the bracket is true, otherwise 0, and (a) is from $\Pr(\bar{s}_{k:n}) = 1/L^{n-k+1}$.

Before we move on further, we introduce a definition and a lemma which are useful for further simplification of (23).

Definition 9: (non-negative correlation) Two random events \mathcal{A} and \mathcal{B} are said to be *non-negatively correlated* if $\text{cov}(I\{\mathcal{A}\}, I\{\mathcal{B}\}) \geq 0$. We use the tilde symbol \sim between two events, i.e., $\mathcal{A} \sim \mathcal{B}$, to imply that the two are *non-negatively correlated*.

Lemma 10: $\mathcal{A} \sim \mathcal{B}$ if and only if $\Pr(\mathcal{A}\mathcal{B}) \geq \Pr(\mathcal{A})\Pr(\mathcal{B})$.

Proof: This can be easily seen by Def. 9. \square

Here we aim to show $I\{d_{k+1}(s_{k+1:n}, \bar{s}_{k+1:n}) \leq C\} \sim I\{\tilde{\Delta}_k(s_k, \bar{s}_k) \leq C\}$. To this end, we first show $I\{d_{k+1} \leq C\} \sim I\{d_1 \leq C\}$, and then $I\{d_1 \leq C\} \sim I\{\tilde{\Delta}_k \leq C\}$, and thus $I\{d_{k+1} \leq C\} \sim I\{\tilde{\Delta}_k \leq C\}$. Before we move on, note the inequalities $d_{k+1} \leq d_1$ and $\tilde{\Delta}_k \leq d_1$ from (3) and (5). Now, we show that $I\{d_{k+1} \leq C\} \sim I\{d_1 \leq C\}$ by showing the following, $\Pr(d_{k+1} \leq C, d_1 \leq C) = \Pr(d_1 \leq C) \geq \Pr(d_{k+1} \leq C)\Pr(d_1 \leq C)$. Thus, the first is shown. Now, for the second, we show that $\Pr(d_1 \leq C, \tilde{\Delta}_k \leq C) = \Pr(d_1 \leq C) \geq \Pr(d_1 \leq C)\Pr(\tilde{\Delta}_k \leq C)$, thus $I\{d_1 \leq C\} \sim I\{\tilde{\Delta}_k \leq C\}$. Therefore,

$I\{d_{k+1}(s_{k+1:n}, \bar{s}_{k+1:n}) \leq C\} \sim I\{\tilde{\Delta}_k(s_k, \bar{s}_k) \leq C\}$; this is also verified through extensive simulations.

Now, return to the discussion of (23). Let $\mathcal{A} := \{\tilde{\Delta}_k(s_k, \bar{s}_k) \leq C\}$ and $\mathcal{B} := \{d_{k+1}(s_{k+1:n}, \bar{s}_{k+1:n}) \leq C\}$. Using Lemma 10, the joint probability $\Pr(\tilde{\Delta}_k(s_k, \bar{s}_k) \leq C, d_{k+1}(s_{k+1:n}, \bar{s}_{k+1:n}) \leq C)$ is lower bounded by $\Pr(\tilde{\Delta}_k(s_k, \bar{s}_k) \leq C)\Pr(d_{k+1}(s_{k+1:n}, \bar{s}_{k+1:n}) \leq C)$.

B. Proof of Lemma 5

$\mathbb{E}[\tilde{\Delta}_k(s_k, \bar{s}_k)]$ is expressed as follows

$$\begin{aligned}
& \mathbb{E} \left[\frac{|\bar{s}_k - s_k + \mathbf{R}_{k,-}^{-1} \tilde{\mathbf{v}}|^2}{\|\mathbf{R}_{k,-}^{-1}\|^2} \right] \\
&= \frac{|\bar{s}_k - s_k|^2}{\mathbb{E}[\|\mathbf{R}_{k,-}^{-1}\|^2]} + \mathbb{E} \left[\frac{\left| \sum_{i=1}^n R_{k,j}^{-1} \cdot \tilde{v}_i \right|^2}{\|\mathbf{R}_{k,-}^{-1}\|^2} \right] + 2(\bar{s}_k - s_k)^* \mathbb{E} \left[\frac{\sum_{i=1}^n R_{k,j}^{-1} \cdot \tilde{v}_i}{\|\mathbf{R}_{k,-}^{-1}\|^2} \right].
\end{aligned}$$

The first term is upper bounded as follows,

$$|\bar{s}_k - s_k|^2 / \mathbb{E}[\|\mathbf{R}_{k,-}^{-1}\|^2] \stackrel{(a)}{\leq} |\bar{s}_k - s_k|^2 \mathbb{E}[\|\mathbf{R}_{k,-}\|^2] \stackrel{(b)}{=} |\bar{s}_k - s_k|^2 \cdot n,$$

where (a) is from $\mathbb{E}[\|\mathbf{R}_{k,-}^{-1}\|^2] \mathbb{E}[\|\mathbf{R}_{k,-}\|^2] \geq \mathbb{E}[\|\mathbf{R}_{k,-}^{-1} \mathbf{R}_{k,-}\|] = 1$ and

(b) is from $\|\mathbf{R}_{k,-}\|^2 = \|\mathbf{Q}^* \mathbf{H}_{k,-}\|^2 = \|\mathbf{H}_{k,-}\|^2$.

The second term becomes σ^2 as follows,

$$\begin{aligned}
& \mathbb{E} \left[\frac{\left| \sum_{i=1}^n R_{k,j}^{-1} \cdot \tilde{v}_i \right|^2}{\|\mathbf{R}_{k,-}^{-1}\|^2} \right] \\
&\stackrel{(c)}{=} \sum_{i=1}^n \mathbb{E} \left[\frac{|R_{k,i}^{-1}|^2}{\|\mathbf{R}_{k,-}^{-1}\|^2} \right] \mathbb{E}[\tilde{v}_i^2] + \sum_{i=1, j=1, i \neq j}^n \mathbb{E} \left[\frac{R_{k,i}^{-1*} R_{k,j}^{-1}}{\|\mathbf{R}_{k,-}^{-1}\|^2} \right] \mathbb{E}[\tilde{v}_i^*] \mathbb{E}[\tilde{v}_j] \\
&= \sigma^2,
\end{aligned}$$

where (c) is from the independence of $\tilde{\mathbf{v}}$ and \mathbf{R}^{-1} .

The third term becomes zero as follows

$$\mathbb{E} \left[\frac{\sum_{i=1}^n R_{k,j}^{-1} \cdot \tilde{v}_i}{\|\mathbf{R}_{k,-}^{-1}\|^2} \right] \stackrel{(d)}{=} \sum_{i=1}^n \mathbb{E} \left[\frac{R_{k,i}^{-1}}{\|\mathbf{R}_{k,-}^{-1}\|^2} \right] \mathbb{E}[\tilde{v}_i] = 0,$$

where (d) is also from the independence of $\tilde{\mathbf{v}}$ and \mathbf{R}^{-1} .

Therefore, $\mathbb{E}[\tilde{\Delta}_k(s_k, \bar{s}_k)] \leq \sigma^2 \left(|\bar{s}_k - s_k|^2 \rho + 1 \right)$.

Now, $\Pr(\tilde{\Delta}_k(s_k, \bar{s}_k) \leq C)$ is lower bounded by as follows,

$$\Pr(\tilde{\Delta}_k(s_k, \bar{s}_k) \leq C) \stackrel{(a)}{\geq} \left(1 - \frac{1}{\alpha n} \left(|\bar{s}_k - s_k|^2 \rho + 1 \right) \right)_+,$$

where (a) is from the Markov inequality and $(\cdot)_+$ is to make sure the probability to be nonnegative.

C. Proof of Lemma 6

$\mathbb{E}[d_{k+1}(s_{k+1:n}, \bar{s}_{k+1:n})]$ is expressed as follows

$$\begin{aligned}
& \mathbb{E} \left[d_{k+1}(\mathbf{s}_{k+1:n}, \bar{\mathbf{s}}_{k+1:n}) \right] \\
&= \sum_{i=k+1}^n \mathbb{E} \left[\left| \sum_{j=i}^n R_{i,j}(\bar{s}_j - s_j) + \tilde{v}_i \right|^2 \right] \\
&\stackrel{(a)}{=} \sum_{i=k+1}^n \sum_{j=i}^n |\bar{s}_j - s_j|^2 \left(\mathbb{E} \left[\|\mathbf{R}_{\rightarrow j}\|^2 \right] - \sum_{i=1}^k \mathbb{E} \left[|R_{i,j}|^2 \right] \right) + (n-k)\sigma^2 \\
&\stackrel{(b)}{=} (n-k) \|\bar{\mathbf{s}}_{k+1:n} - \mathbf{s}_{k+1:n}\|^2 + (n-k)\sigma^2,
\end{aligned}$$

where (a) is from the independence between $\tilde{\mathbf{v}}$ and \mathbf{R} , and the fact that any off-diagonal element of \mathbf{R} has mean zero [24], (b)

is from $\|\mathbf{R}_{\rightarrow j}\|^2 = \|\mathbf{H}_{\rightarrow j}\|^2$.

Finally, using the Markov inequality,

$$\Pr(d_{k+1}(\mathbf{s}_{k+1:n}, \bar{\mathbf{s}}_{k+1:n}) \leq C) \geq \left(1 - \frac{n-k}{\alpha n} \left(\|\bar{\mathbf{s}}_{k+1:n} - \mathbf{s}_{k+1:n}\|^2 \frac{\rho}{n} + 1 \right) \right)_+.$$

D. Proof of Theorem 7

$$\begin{aligned}
& \mathbb{E}[N_k^{cc} N_{k+1}^{sc}] \\
&\stackrel{(a)}{\geq} (1/L^{n-k+1}) \sum_{s_k} \sum_{\bar{s}_k} \left(1 - \frac{1}{\alpha n} \left(|\bar{s}_k - s_k|^2 \rho + 1 \right) \right)_+ \\
&\cdot \sum_{s_{k+1:n}} \sum_{\bar{s}_{k+1:n}} \left(1 - \frac{n-k}{\alpha n} \left(\|\bar{\mathbf{s}}_{k+1:n} - \mathbf{s}_{k+1:n}\|^2 \frac{\rho}{n} + 1 \right) \right)_+ \\
&\stackrel{(b)}{=} L^{n-k+1} \cdot \left(1 - \frac{1}{\alpha n} \left(\mathbb{E} \left[|\bar{s}_k - s_k|^2 \right] \rho + 1 \right) \right)_+ \\
&\cdot \left(1 - \frac{n-k}{\alpha n} \left(\mathbb{E} \left[|\bar{s}_k - s_k|^2 \right] \frac{n-k}{n} \rho + 1 \right) \right)_+,
\end{aligned}$$

where (a) is from Lemma 4, 5 and 6, (b) is from

$$\left(\sum_k a_k \right)_+ \leq \sum_k (a_k)_+, \quad \mathbb{E} \left[|\bar{s}_k - s_k|^2 \right] = \frac{1}{L^2} \sum_{s_k} \sum_{\bar{s}_k} |\bar{s}_k - s_k|^2,$$

$$\sum_{\bar{s}_{k+1:n}} \sum_{s_{k+1:n}} 1 = L^{2(n-k)}, \quad \text{and} \quad \mathbb{E} \left[\|\bar{\mathbf{s}}_{k+1:n} - \mathbf{s}_{k+1:n}\|^2 \right]$$

$$= \frac{1}{L^{2(n-k)}} \sum_{\bar{s}_{k+1:n}} \sum_{s_{k+1:n}} \|\bar{\mathbf{s}}_{k+1:n} - \mathbf{s}_{k+1:n}\|^2.$$

$\mathbb{E}[N_{k+1}^{sc}]$ can be easily derived using a similar procedure.

REFERENCES

- [1] U. Fincke and M. Pohst, "Improved methods for calculating vectors of short length in a lattice, including a complexity analysis," *Math. Computation*, vol. 44, no. 2, pp. 463–471, Apr. 1985.
- [2] E. Agrell, T. Eriksson, A. Vardy, and K. Zeger, "Closest point search in lattices," *IEEE Trans. on Inf. Theory*, vol. 48, no. 8, pp. 2201–2214, Aug. 2002.
- [3] E. Viterbo and J. Boutros, "A universal lattice code decoder for fading channels," *IEEE Trans. on Inf. Theory*, vol. 45, no. 5, pp. 1639–1642, July 1999.
- [4] M. O. Damen, H. El Gamal, and G. Caire, "On maximum-likelihood detection and the search for the closest lattice point," *IEEE Trans. on Inf. Theory*, vol. 49, no. 10, pp. 2389–2402, Oct. 2003.
- [5] D. Pham, K. R. Pattipati, P. K. Willett, and J. Luo, "An Improved Complex Sphere Decoder for V-BLAST Systems," *IEEE Signal Processing Letters*, vol. 11, no. 9, pp. 748–751, Sep. 2004.
- [6] R. S. Mozes, and M. J. F.-G. Garcia, "Efficient Complex Sphere Decoding for MC-CDMA Systems," *IEEE Trans. on Wireless Communications*, vol. 5, no. 11, pp. 2992–2996, Nov. 2006.
- [7] R. Kobayashi, T. Kawamura, N. Miki, and M. Sawahashi, "Throughput Comparisons of Star 32/64 QAM Schemes Based on Mutual Information Considering Cubic Metric," *International Conference on Wireless Communications and Signal Processing (WCSP)*, Nanjing, China, Nov. 2011.
- [8] G. D. Forney and G. Ungerboeck, "Modulation and Coding for Linear Gaussian Channels," *IEEE Trans. on Inf. Theory*, vol. 44, no. 6, pp. 2284–2415, Oct. 1998.
- [9] I. Nevat, G. W. Peters, and J. Yuan, "Detection of Gaussian Constellations in MIMO Systems Under Imperfect CSI," *IEEE Trans. on Communications*, vol. 58, no. 4, pp. 1151–1160, Apr. 2010.
- [10] A. Burg, M. Borgmann, M. Wenk, M. Zellweger, W. Fichtner, and H. Bölcskei, "VLSI implementation of MIMO detection using the sphere decoding algorithm," *IEEE Journal of Solid-State Circuits*, vol. 40, no. 7, pp. 1566–1577, July 2005.
- [11] B. M. Hochwald and S. ten Brink, "Achieving near-capacity on a multiple-antenna channel," *IEEE Trans. on Communications*, vol. 51, no. 3, pp. 389–399, Mar. 2003.
- [12] C. Hess, M. Wenk, A. Burg, P. Luethi, C. Studer, N. Felber, and W. Fichtner, "Reduced-Complexity MIMO Detector with Close-to ML Error Rate Performance," *Proc. 17th ACM Great Lakes symposium on VLSI*, Italy, Mar. 2007.
- [13] B. Mennenga and G. Fettweis, "Search sequence determination for tree search based detection algorithms," *IEEE Sarnoff Symposium, SARNOFF'09*, USA, Mar. 2009.
- [14] L. G. Barbero and J. S. Thompson, "Fixing the Complexity of the Sphere Decoder for MIMO detection," *IEEE Trans. on Wireless Communications*, vol. 7, no. 6, pp. 2131–2142, June 2008.
- [15] M. Wenk, L. Bruderer, A. Burg, C. Studer, "Area-and Throughput-Optimized VLSI Architecture of Sphere Decoding," *18th IEEE/IFIP VLSI System on Chip Conference*, Spain, Sep. 2010.
- [16] M. Stojnic, H. Vikalo, and B. Hassibi, "Speeding up the Sphere Decoder With H^∞ and SDP inspired Lower Bounds," *IEEE Trans. on Signal Processing*, vol. 56, no. 2, pp. 712–726, Feb. 2008.
- [17] S. Barik and H. Vikalo, "Sparsity-Aware Sphere Decoding: Algorithms and Complexity Analysis," *IEEE Trans. on Signal Processing*, vol. 62, no. 9, pp. 2212–2225, May. 2014.
- [18] R. Gowaikar and B. Hassibi, "Statistical Pruning for Near-Maximum Likelihood Decoding," *IEEE Trans. on Signal Processing*, vol. 55, no. 6, pp. 2661–2675, June 2007.
- [19] B. Shim and I. Kang, "Sphere decoding with a probabilistic tree pruning," *IEEE Trans. on Signal Processing*, vol. 56, no. 10, pp. 4867–4878, Oct. 2008.
- [20] J. Ahn, H.-N. Lee, and K. Kim, "A Near-ML Decoding with Improved Complexity over Wider Ranges of SNR and System Dimension in MIMO Systems," *IEEE Trans. on Wireless Communications*, vol. 11, no. 1, pp. 33–37, Jan. 2012.
- [21] L. Ma, K. Dickson, J. McAllister, and J. McCanny, "QR Decomposition-Based Matrix Inversion for High Performance Embedded MIMO Receivers," *IEEE Trans. on Signal Processing*, vol. 59, no. 4, pp. 1858–1867, Apr. 2011.
- [22] J. Jaldén and B. Ottersten, "On the complexity of Sphere Decoding in Digital Communications," *IEEE Trans. on Signal Processing*, vol. 53, no. 4, pp. 1474–1484, Apr. 2005.
- [23] H. Vikalo and B. Hassibi, "On the Sphere-Decoding Algorithm II. Generalizations, Second-Order Statistics, and Applications to Communications," *IEEE Trans. on Signal Processing*, vol. 53, no. 8, pp. 2819–2834, Aug. 2005.
- [24] B. Hassibi and H. Vikalo, "On the Sphere-Decoding Algorithm I. Expected Complexity," *IEEE Trans. on Signal Processing*, vol. 53, no. 8, pp. 2806–2818, Aug. 2005.
- [25] D. Seethaler and H. Bölcskei, "Performance and Complexity Analysis of Infinity-Norm Sphere-Decoding," *IEEE Trans. on Inf. Theory*, vol. 56, no. 3, pp. 1085–1105, Mar. 2010.